

https://dspace.org/

Ascending Vaginal Infection in Mice Induces Preterm Birth and Neonatal Morbidity

A. K Boyle; K Tetorou; N Suff; L Beecroft; Simon Waddington ...

ELSEVIER SCIENCE INC
https://hdl.handle.net/10539/47415
WOS

Downloaded from a DSpace repository. https://dspace.org/

The American Journal of Pathology, Vol. 195, No. 5, May 2025

ELSEVIER

The American Journal of
PATHOLOGY
ajp.amjpathol.org

IMMUNOPATHOLOGY AND INFECTIOUS DISEASES

Ascending Vaginal Infection in Mice Induces Preterm Birth and Neonatal Morbidity

Check for updates

Ashley K. Boyle,* Konstantina Tetorou,* Natalie Suff,† Laura Beecroft,* Margherita Mazzaschi,* Rajvinder Karda,* Mariya Hristova,* Simon N. Waddington,*‡ and Donald Peebles*

From the Elizabeth Garrett Anderson Institute for Women's Health, University College London, London, United Kingdom; the Department of Women and Children's Health,† St Thomas' Hospital, King's College London, London, United Kingdom; and the Faculty of Health Sciences,‡ Wits/South African Medical Research Council Antiviral Gene Therapy Research Unit, Johannesburg, South Africa*

Accepted for publication January 10, 2025.

Address correspondence to Ashley K. Boyle, Ph.D., Elizabeth Garrett Anderson Institute for Women's Health, University College London, 86-96 Chenies Mews, London, WC1E 6HX, United Kingdom.
E-mail: ashley.boyle@ucl.ac.uk.

Preterm birth (PTB; delivery before 37 weeks), the main cause of neonatal death worldwide, can lead to adverse neurodevelopmental outcomes, as well as lung and gut pathology. PTB can be associated with ascending vaginal infection. Ascending *Escherichia coli* infection in pregnant mice induces PTB and reduces pup survival. The current study demonstrated that this model recapitulates the pathology observed in human preterm neonates (namely, neuroinflammation, lung injury, and gut inflammation). In neonatal brains, there is widespread cell death, microglial activation, astrogliosis, and reduced neuronal density. The utility of this model was validated by assessing the efficacy of maternal cervical gene therapy with an adeno-associated viral vector containing human β defensin 3. This improved pup survival and reduced tumor necrosis factor alpha mRNA expression in perinatal pup brains exposed to *E. coli*. This model provides a unique opportunity to evaluate the therapeutic benefit of preterm labor interventions on perinatal pathology. *(Am J Pathol 2025, 195: 891–906; https://doi.org/10.1016/j.ajpath.2025.01.008)*

Preterm birth (PTB; delivery before 37 weeks) is the leading cause of neonatal morbidity and mortality worldwide.[1,2] This is a serious global health problem, affecting approximately 11% of all pregnancies and 15 million babies a year.[3–5] Risk factors include extremes in maternal age, body mass index, socioeconomic disadvantage, smoking, multiple pregnancies, and a previous PTB.[6,7]

Despite extensive research, treatment strategies have proved largely ineffective. This is likely because of the multifactorial nature of spontaneous PTB. The cervix, a physical and immunologic barrier containing immune cells and producing antimicrobial peptides, plays a key role in preventing bacterial invasion. However, at least 40% of spontaneous PTBs are associated with microbes, which are thought to ascend from the vagina into the uterus, via the cervix.[8] The microorganisms commonly linked with PTB have relatively low pathogenicity, and cases of chorioamnionitis are mostly polymicrobial. Species of *Mycoplasma*, *Ureaplasma*, *Fusobacterium*, and *Streptococcus* have been found in the amniotic fluid in those most at risk.[9,10] Vaginal *Lactobacillus iners* dominance has been linked to PTB risk in a UK population, whereas *Lactobacillus crispatus* dominance has been associated with term delivery.[11–13]

The fetal immune system is primed *in utero* through exposure of the placenta, lungs, gut, and skin to microbes, as well as the vertical transmission of maternal immune cells.[14,15] When delivered, babies exposed to infection/inflammation have an increased risk of periventricular leukomalacia, intraventricular hemorrhage, and early-onset neonatal sepsis. These conditions increase the likelihood of long-term complications resulting in neurodevelopmental disorders, such as cerebral palsy, and respiratory-related conditions, such as bronchopulmonary dysplasia, and necrotizing enterocolitis (NEC).[16,17]

Supported by Action Medical Research and Borne grant GN2647 (N.S., S.N.W., and D.P.); and Wellbeing of Women grant RG2365 (A.K.B., N.S., R.K., M.H., S.N.W., and D.P.).

Copyright © 2025 American Society for Investigative Pathology. Published by Elsevier Inc.
This is an open access article under the CC BY license (*http://creativecommons.org/licenses/by/4.0*).
https://doi.org/10.1016/j.ajpath.2025.01.008

PTB can be induced in mice by ascending vaginal infection with a pathogenic *Escherichia coli* strain associated with human neonatal meningitis. The proportion of pups born alive is reduced and, in surviving pups, there is evidence of neuroinflammation.[18] This model was used to investigate a novel therapeutic, demonstrating that adeno-associated viral (AAV) vector gene therapy to increase levels of the antimicrobial peptide human β defensin 3 (HBD3) in the cervix can reduce ascending infection and improve pup survival.[19]

Here, the fetal and neonatal outcomes following exposure to ascending vaginal infection were characterized, assessing the fetal lungs and gut, as well as further interrogating fetal and neonatal neuropathology. The impact of pre-treating dams with cervical HBD3 gene therapy on perinatal neuroinflammation was assessed.

Materials and Methods

AAV Vector Production

An AAV8 bicistronic vector was produced, encapsidating a single-stranded DNA sequence containing the HBD3 gene followed by the engineered green fluorescent protein (eGFP) gene, each under the transcriptional activity of a separate cytomegalovirus (CMV) promotor. An AAV8 vector containing CMV-eGFP was used as a vehicle control. For NF-κB biosensor experiments, an AAV8 serotype vector containing a minimal promoter upstream of the NF-κB response element, followed by a firefly luciferase and 2A-eGFP transgene, was developed.[20]

AAV production and purification followed standard procedures. Briefly, HEK293T cells were transfected with pAAV-CMV-hDEFB103B-CMV-eGFP or pAAV-CMV-eGFP (Vector Biolabs, Malvern, PA), using polyethylenimine (PEImax; Polysciences Inc., Warrington, PA). Cells were incubated at 37°C for 72 hours, then collected, centrifuged, and freeze thawed in lysis buffer. Both cell supernatant and cell lysate were benzonase treated, then clarified via centrifugation and 0.22-μm filtration before purification. AAVs were purified by high-performance liquid chromatography (ÄKTAprime plus; GE Healthcare, Buckinghamshire, UK) with a POROS CaptureSelect AAV Resin (Thermo Fisher Scientific, Oxford, UK) column. Purified vector fractions were dialyzed against phosphate-buffered saline (PBS) overnight (Slide-A-lyzer dialysis cassette 10,000 MWCO; Thermo Fisher Scientific). Viral genome titers were quantified by quantitative PCR (qPCR).

Mouse Model of Ascending Vaginal Infection

All animal studies were conducted under a UK Home Office Licence (PAD4E6357) in line with the Animal Scientific Procedures Act (1986) and following the Animal Research: Reporting of In Vivo Experiments (ARRIVE) guidelines 2.0.[21] Temperature (19°C to 23°C) and humidity (approximately 55%) were tightly controlled at all times, with constant 12-hour light/dark cycles. Virgin female C57BL/6 Tyr^{c-2J} mice (Charles River, Kent, UK), aged 6 to 12 weeks, were time mated [embryonic day (E) 0.5, designated when vaginal plug was found].

On E16.5, mice were anesthetized by the inhalation of isoflurane (5% for induction, 1.5% for maintenance in oxygen). *E. coli* K1 A192PP-*lux2*, modified to contain the lux operon from *Photorhabdus luminescens*,[22] was delivered intravaginally to induce preterm delivery, as previously described.[18] Briefly, 20 μL of midlogarithmic-phase *E. coli* ($1 \times 10^{2-3}$ colony-forming units resuspended in PBS) or PBS (vehicle control) was delivered into the vagina of pregnant mice using a 200-μL pipette tip, followed by 20 μL of 20% Pluronic F-127 gel (Sigma-Aldrich, Dorset, UK) to prevent leakage. Animals were allowed to recover from anesthesia, then caged individually and monitored by closed-circuit television for signs of labor and the delivery of pups. Time to delivery was recorded as the number of hours from the time of intravaginal administration of *E. coli* or PBS to the delivery of the first pup. The number of live/dead pups was recorded within 24 hours of their delivery and a percentage calculated per litter.

In a separate cohort, on the day of birth, AAV8 containing a firefly luciferase reporter driven by the NF-κB response elements was administered intracranially to neonatal mice exposed to *E. coli* or PBS *in utero*. Neonatal mice were imaged daily up to 21 days old to assess NF-κB response in the brain.

In a third cohort, pregnant C57BL/6 Tyr^{c-2J} females (aged 6 to 12 weeks) were anesthetized on E13.5, and 10 μL of AAV8-HBD3 or AAV8-GFP was delivered intravaginally using a sterile 200-μL pipette tip (1×10^{12} genomic copies/mL diluted in PBS), followed by 10 μL of AK012 thermosensitive gel (PolySciTech, West Lafayette, IN). Administration of *E. coli* or PBS on E16.5 was then performed as already described.

Bioluminescent Imaging

Mice were imaged for 2 minutes using a cooled charged-coupled device camera (IVIS Lumina; Perkin Elmer, Coventry, UK). Dams were anesthetized with isoflurane as above.

Tissue Collection and Processing

Perinatal pups were sacrificed by decapitation on E18.5 (48 hours after intravaginal infection) to harvest brain, lungs, and gut (one to three pups per litter collected from the right horn). Dams and postnatal day (P) 7 and P14 pups were anesthetized using isoflurane, the right atrium was incised, and PBS was injected into the left ventricle. P7 brains were cut into three coronal sections: the forebrain, the mid brain region, and the hindbrain/cerebellum. Tissues for qPCR and enzyme-linked immunosorbent assay analyses were snap

frozen and stored at −80°C until required. For immunohistochemistry, brain and lung samples were fixed in 4% paraformaldehyde for 24 to 48 hours, then stored in 30% sucrose at 4°C. Tissues were frozen on dry ice and a cryostat (LEICA CM1900; Leica, Newcastle upon Tyne, UK) was used at −20°C to cut 50 serial sections (40 μm thick) of the tissues, beginning from the fusion of the corpus callosum of the brain. Frozen sections were stored at −80°C.

RNA Extraction, cDNA Synthesis, and qPCR

Total RNA was extracted from E18.5 brains, lungs, and gut and P7 forebrain and mid brain samples by RNAeasy mini kit (Qiagen, Germantown, MD), according to the manufacturer's instructions, and quantified on a FLUOstar Omega Microplate Reader (BMG Labtech Ltd, Aylesbury, UK). RNA (400 ng) was reverse transcribed using the High Capacity cDNA Reverse Transcription Kit (Thermo Fisher Scientific). For qPCR, primers for glyceraldehyde-3-phosphate dehydrogenase (forward: 5′-ACGGCAAATT CAACGGCAC-3′; reverse: 5′-TAGTGGGGTCTCGCTC CTGG-3′) and Il1b (forward: 5′-AACCTGCTGGTGTGTG ACGTTC-3′; reverse: 5′-CAGCACGAGGCTTTTTTGTT GT-3′) were designed and purchased from Integrated DNA Technologies (Leuven, Belgium), or predesigned TaqMan gene expression assays were used (Thermo Fisher Scientific) (Table 1). All qPCR analyses were performed on a QuantStudio 6 Flex Real-Time PCR System (Applied Biosystems, Thermo Fisher Scientific). Target mRNA expression was normalized for RNA loading using glyceraldehyde-3-phosphate dehydrogenase (Integrated DNA Technologies), and the mRNA concentration in each sample was calculated relative to the vehicle control group (PBS or AAV8-GFP + PBS) using the $2^{-\Delta\Delta C_T}$ method of analysis.

Enzyme-Linked Immunosorbent Assay

E18.5 brains were homogenized in lysis buffer (radioimmunoprecipitation assay buffer; Merck Millipore, Darmstadt, Germany) containing 1 Complete Protease Inhibitor Cocktail Tablet (Roche, Basel, Switzerland) using a Tissue Lyser II (Qiagen) at 30 Hz. The samples were incubated on ice for 5 minutes and then centrifuged at 10,000 × *g* for 10 minutes at 4°C. The lysates were stored at −80°C. Total protein was quantified by using the DC protein assay (Bio-Rad, Hercules, CA), according to the manufacturer's instructions. The V-PLEX Proinflammatory Panel 1 Mouse Kit (Meso Scale Diagnostics, Rockville, MD) was used to quantify inflammatory mediator secretion, according to the manufacturer's guidelines, and measured on a Meso Sector S 600 mm. For E18.5 lungs and gut, total protein quantification was performed using the Pierce BCA Protein Assay kit (Thermo Fisher Scientific), then the MILLIPLEX mouse cytokine/chemokine magnetic bead panel (Luminex Multiplex Assay; R&D Systems, Minneapolis, MN) was used according to the manufacturer's guidelines and measured on a Luminex instrument with xPONENT software (Diasorin, Saluggia, Italy).

Table 1 Predesigned TaqMan Gene Expression Assays

Gene	TaqMan assay identifier
Cxcl1	Mm04207460_m1
Cxcl2	Mm00436450_m1
Gfap	Mm01253033_m1
Iba1	Mm00520165_m1
Il6	Mm00446190_m1
Spa	Mm00499170_m1
Spb	Mm00455678_m1
Spc	Mm00488144_m1
Spd	Mm00486060_m1
Tnfa	Mm00443258_m1

Histology and Immunohistochemistry

Histologic staining included terminal transferase-mediated dUTP nick end labeling (TUNEL) with Co/Ni enhancement (Roche) performed following manufacturer's instructions, cresyl-violet (Nissl) staining, and hematoxylin and eosin staining. For brain histology and immunohistochemistry, five sections per brain (400 μm apart) were rehydrated in distilled water and left to dry. Immunohistochemical staining was performed as previously described.[23] Briefly, tissue sections were incubated overnight with the following primary antibodies: rabbit polyclonal anti−glial fibrillary acidic protein (GFAP; 1:6000; Dako; Agilent Technologies, Inc., Santa Clara, CA), rabbit polyclonal anti−allograft inflammatory factor 1 (IBA1; microglia; 1:2000; Wako Company, Tokyo, Japan), rabbit anti−myelin basic protein (MBP; 1:200; Abcam, Cambridge, UK), or mouse monoclonal anti-neuronal nuclei (NeuN; 1:15,000; Merck Millipore). The following day, sections were incubated with either biotinylated goat anti-rabbit or anti-rat (1:100; Vector Laboratories, Newark, CA) secondary antibodies for 1 hour, then incubated with Avidin-Biotinylated horseradish peroxidase complex (Vector Laboratories), followed by diaminobenzidine/hydrogen peroxide (Thermo Fisher Scientific).

For lung analyses, two or three sections of lung per fetus or neonate (400 μm apart) were rehydrated in distilled water, then stained with Nissl, or immunohistochemical labeling was performed as above with anti-mouse lymphocyte antigen 6 complex locus G6D (Ly6G) primary antibody (BioLegend, London, UK) and goat anti-rabbit secondary antibody.

Histologic Assessments

Assessments were performed on the following regions: cortex, pyriform cortex, external capsule, striatum, hippocampus, and thalamus. The corpus callosum was analyzed

for E18.5 brains in addition to or in place of the external capsule.

Optical Luminosity

Optical luminosity values were generated to measure reactive astrogliosis and myelination through GFAP and myelin basic protein immunoreactivity, respectively. All regions were assessed for GFAP, and the striatum and external capsule were assessed for MBP. Images were captured in three optical fields using a Sony (Tokyo, Japan) AVT-Horn 184 3CCD camera [×20 magnification; 24-bit red, green, and blue (RGB); 760 × 570-pixel resolution], then imported into Optimas 6.51 (Media Cybernetics Inc., Rockville, MD) to determine the mean and SD of the optical luminosity value. To obtain the intensity of the staining for each image, the SD was subtracted from the mean optical luminosity value, and the resulting values were normalized by subtracting the optical luminosity value of the glass surrounding the tissue section.[24]

Ramification Index

IBA1-positive microglial cell bodies and branch density were assessed using a 0.049 × 0.049-mm square grid (×40 magnification) placed in three fields for all brain regions. The number of cell bodies within the grid were counted (C), and the average number of branches crossing the three horizontal and three vertical 0.49-mm gridlines was calculated (B). The microglial ramification index was calculated as follow: B^2/C.

Stereology for Brain and Lung Tissues

TUNEL- (×20 magnification), NeuN- (×40 magnification), and Ly6G-positive cells (×40 magnification) were manually counted using ImageJ software version 1.53 (NIH, Bethesda, MD; *https://imagej.net*). Brain width, cortex thickness, hippocampal area, and lung airspace area were measured using the free-hand tool (×40 magnification). Three optical fields were assessed per brain region/lung tissue section, and an average was found.

Statistical Analysis

Data were analyzed by using GraphPad Prism version 8 (GraphPad Software, La Jolla, CA). Time to delivery was analyzed by an unpaired *t*-test with Welsh correction or one-way analysis of variance with Sidak multiple comparisons test. The percentage data for live-born pups were analyzed by performing an arcsine transformation on the proportions, to normalize the binomial distribution, followed by an unpaired *t*-test with Welsh correction or one-way analysis of variance with Sidak multiple comparisons test. Pup survival was analyzed by the log-rank (Mantel-Cox) test. qPCR data were analyzed using an unpaired *t*-test with Welsh correction or one-way analysis of variance with Tukey multiple comparisons test. All enzyme-linked immunosorbent assay data were log transformed, followed by unpaired *t*-tests with Welsh correction. For the NF-κB biosensor data, the area under the curve was calculated, followed by an unpaired *t*-test. For histology and immunohistochemistry, either a *U*-test or multiple *t*-tests with Welsh correction were used. Scoring for histology and immunohistochemistry was blinded where possible. Experimental numbers were based on a sample size calculation that estimated that a minimum of five pups were needed to determine statistically significant differences between groups. Fetal and neonatal tissues were analyzed from a minimum of five independent litters per treatment group. $P < 0.05$ was considered statistically significant.

Results

Ascending Vaginal Infection with *E. coli* Reduces Gestational Length, the Percentage of Pups Born Alive, and Pup Survival over 7 Days

On E16.5, 1×10^2 colony-forming units of bioluminescent *E. coli* or 20 μL PBS control was administered to dams intravaginally. Imaging showed the ascension of the bacteria from the vagina into the uterus within 24 to 48 hours, (Figure 1A). Gestational length was significantly reduced in *E. coli*—treated dams compared with PBS-treated dams (Figure 1B) (mean time to delivery, 40.3 ± 7 versus 52.7 ± 12.9 hours for *E. coli* and PBS groups, respectively; $P = 0.018$). The average percentage of pups born alive was reduced by almost 30% following *E. coli* exposure (71.4% ± 34% versus 100% ± 0% in the PBS group; $P = 0.001$; Figure 1C), and postnatal survival over 7 days was also reduced ($P < 0.0001$; Figure 1D).

Exposure to Ascending Vaginal Infection *in Utero* Induces Perinatal Neuroinflammation

On E18.5, 48 hours after maternal vaginal infection with *E. coli*, perinatal pup tissues were collected and assessed for inflammation and pathology. Inflammatory mediator mRNA expression was up-regulated with *E. coli* exposure (Figure 2A): tumor necrosis factor alpha (Tnfa) ($P = 0.025$), Il1b ($P = 0.01$), and Il6 ($P = 0.034$). TNFA secretion was also significantly elevated (Figure 2B) (0.6 ± 0.2 versus 4.9 ± 12.3 pg/mL in PBS and *E. coli* pups, respectively; $P = 0.003$). The secretion of IL-1B, IL-2, IL-4, IL-5, IL-6, IL-10, CXCL1, and interferon gamma (IFNG) was unchanged (Figure 2B and Supplemental Figure S1A).

Histologic analyses suggested a trend toward $TUNEL^+$ cell death, particularly in the corpus callosum and striatum (Supplemental Figure S1B), and trends for reduced microglial ramification were seen in the cortex and thalamus (Supplemental Figure S1C). The average numbers of $NeuN^+$ neurons in the cortex and hippocampus were not altered by *E. coli* exposure at this time point, and morphologic changes were not observed (Supplemental Figure S1, D—G).

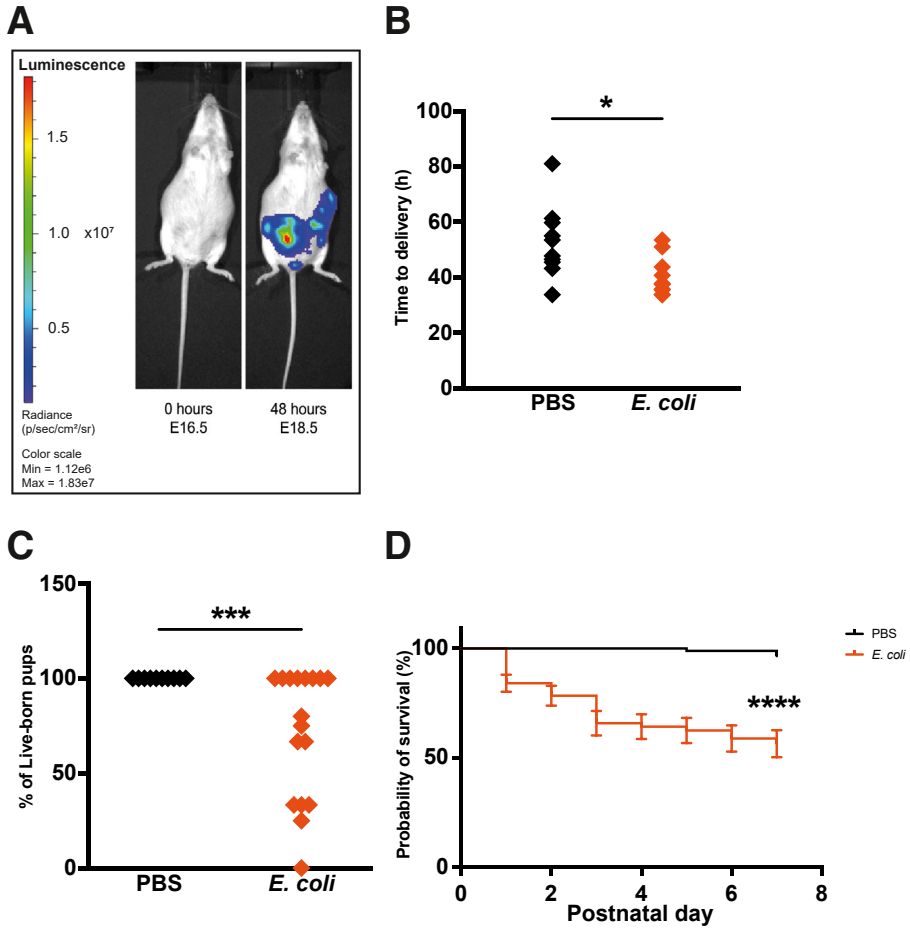

Figure 1 *Escherichia coli* ascends from the vagina into uterus to induce preterm birth and reduce pup survival. **A:** After 48 hours, bioluminescent *E. coli* was visible in the uterus. **B**–**D:** *E. coli* reduced the time to delivery (**B**), the percentage of live-born pups (**C**), and the long-term survival of pups (**D**). $n = 8$ to 10 litters per group (**B**); $n = 10$ to 17 litters per group (**C**); $n = 10$ to 12 litters per group (**D**). $^{*}P < 0.05$, $^{***}P < 0.001$, and $^{****}P < 0.0001$. E, embryonic day; Max, maximum; Min, minimum; PBS, phosphate-buffered saline.

E. coli Exposure *in Utero* Leads to Neonatal Neuropathology

At P7, Il1b and Iba1 mRNA, a marker of microglia, were up-regulated in the forebrain region ($P = 0.001$ and $P = 0.016$, respectively) (Figure 3A). In the mid brain region, mRNA expression was down-regulated (Figure 3B): Tnfa ($P < 0.0001$), Il1b ($P < 0.0001$), Il6 ($P = 0.028$), Cxcl1 ($P = 0.005$), Iba1 ($P < 0.0001$), and Gfap ($P = 0.0006$). Luciferase expression, signifying NF-κB brain signaling, was also reduced in the *E. coli* neonatal brains ($P = 0.002$) (Supplemental Figure S2, A and B).

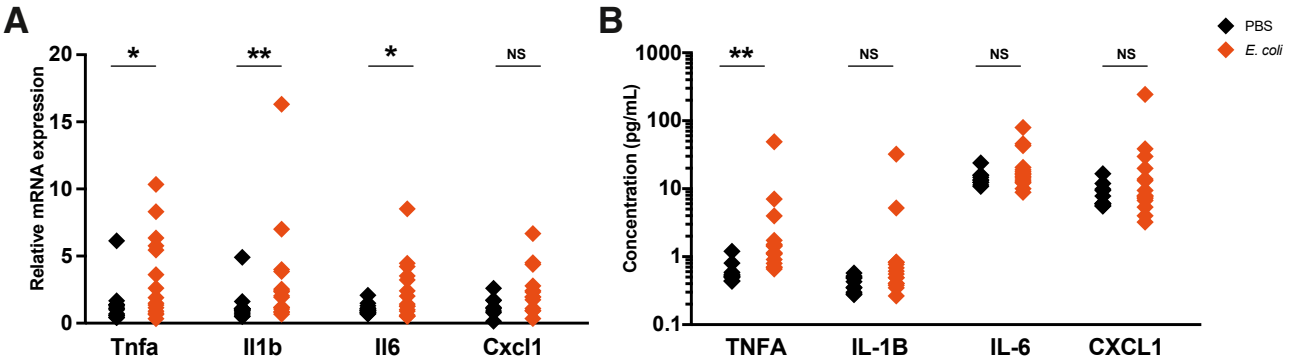

Figure 2 Ascending *Escherichia coli* infection leads to perinatal neuroinflammation 48 hours after exposure. Proinflammatory mediators tumor necrosis factor alpha (Tnfa), Il1b, and Il6 were up-regulated at the mRNA level (**A**), and TNFA was up-regulated at the protein level (**B**), in the perinatal pup brain following maternal *E. coli* infection. Tnfa, Il1b, and Il6: $n = 15$ from 5 litters per group; cxcl1: $n = 8$ to 13 from 5 litters per group (**A**); protein: phosphate-buffered saline (PBS) $n = 10$ from 5 litters; *E. coli* $n = 15$ from 5 litters (**B**). $^{*}P < 0.05$, $^{**}P < 0.01$. NS, nonsignificant.

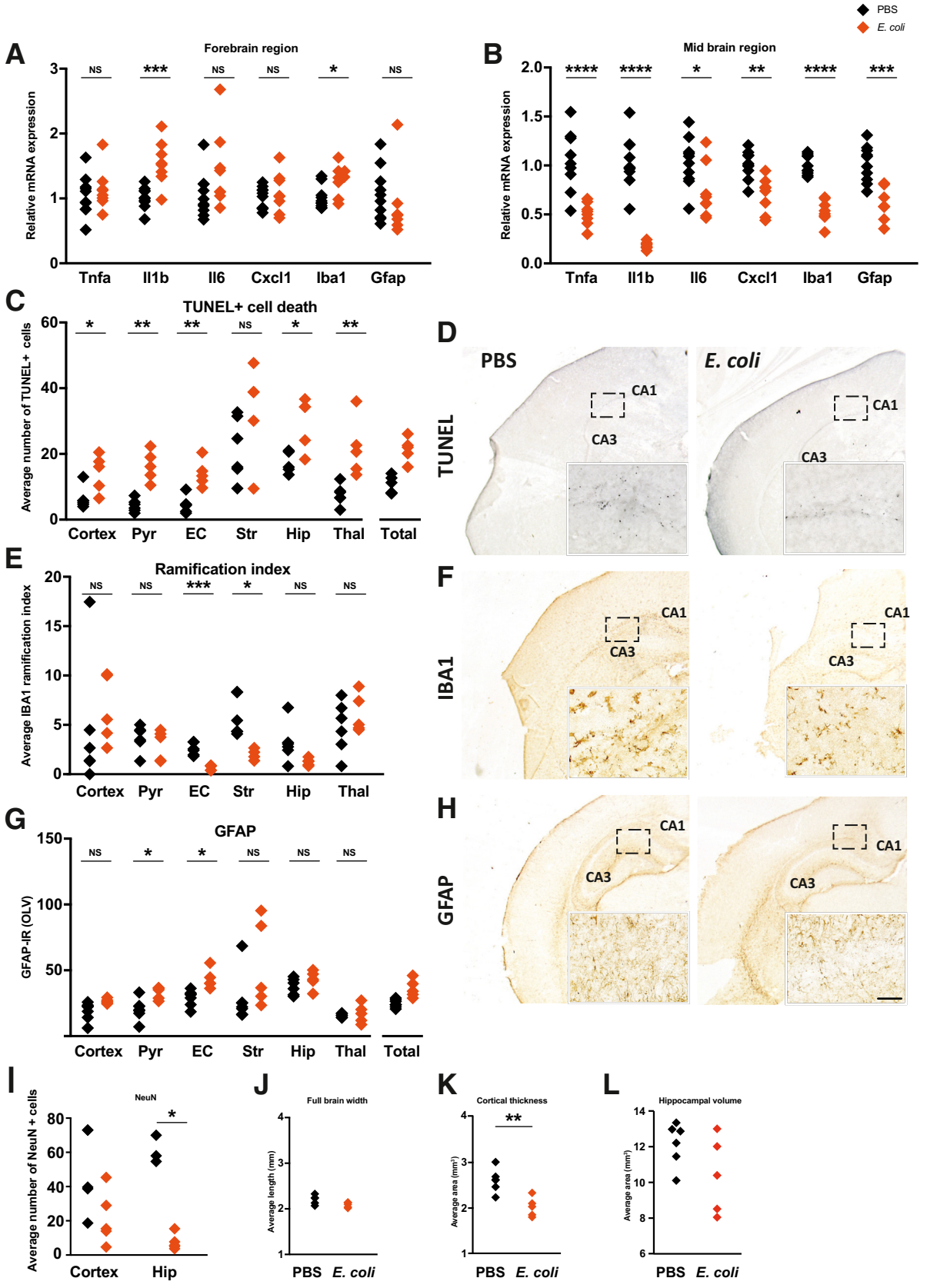
A
Forebrain region
Relative mRNA expression
NS
***
NS
NS
*
NS
Tnfa
Il1b
Il6
Cxcl1
Iba1
Gfap
B
Mid brain region
PBS
E. coli
****
****
*
**
****
***
C
TUNEL+ cell death
Average number of TUNEL+ cells
Cortex
Pyr
EC
Str
Hip
Thal
Total
D
PBS
E. coli
TUNEL
CA1
CA3
E
Ramification index
Average IBA1 ramification index
F
IBA1
G
GFAP
GFAP-IR (OLV)
H
I
NeuN
Average number of NeuN + cells
J
Full brain width
Average length (mm)
K
Cortical thickness
Average area (mm²)
L
Hippocampal volume

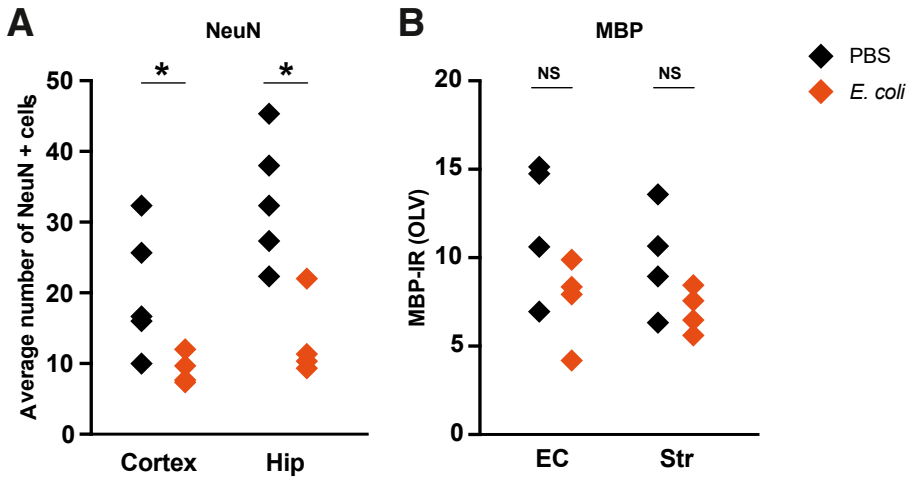

Figure 4 Neuronal density is reduced at postnatal day 14 following *in utero Escherichia coli* exposure. **A:** The average number of neuronal nuclei $(NeuN)^+$ cells was reduced in the cortex and hippocampus (Hip). **B:** There was no significant change to myelin basic protein (MBP) luminosity. $n = 4$ to 5 per group from ≥4 litters (**A** and **B**). $^*P < 0.05$. EC, external capsule; IR, immunoreactivity; NS, nonsignificant; OLV, optical luminosity value; PBS, phosphate-buffered saline; Str, striatum.

Histologic analyses found widespread $TUNEL^+$ cell death in *E. coli* pup brains: cortex ($P = 0.013$), pyriform cortex ($P = 0.004$), external capsule ($P = 0.004$), hippocampus ($P = 0.019$), and thalamus ($P = 0.004$) (Figure 3, C and D). There was reduced microglial ramification (Figure 3, E and F) in the external capsule ($P = 0.001$) and striatum ($P = 0.011$). GFAP, a marker of astrogliosis, was significantly increased in the pyriform cortex (Figure 3, G and H) ($P = 0.027$) and external capsule ($P = 0.027$). *E. coli*—exposed pups also had reduced numbers of $NeuN^+$ neurons in the hippocampal region of the brain (Figure 3I) ($P = 0.036$), and the cortical area was reduced in these pups (Figure 3K) ($P = 0.009$). There was no difference in fetal brain width (Figure 3J) or in hippocampal volume (Figure 3L).

At P14, neuronal density was reduced in the cortex (Figure 4A) ($P = 0.032$) and the hippocampus ($P = 0.016$). There was no longer evidence of $TUNEL^+$ cell death or astrogliosis, and MBP staining intensity was not significantly altered (Figure 4B and Supplemental Figure S2, C and D).

Exposure to Ascending Vaginal Infection *in Utero* Induces Inflammation in the Perinatal Lungs and Gut

Lung

Surfactant protein (Sp) mRNA expression was down-regulated in the lungs of pups from *E. coli*—treated dams (Figure 5A): Spa ($P = 0.023$), Spb ($P = 0.034$), and Spc ($P = 0.006$). There was also pup-dependent elevation of inflammatory mediator mRNA expression but, overall, there was no significant change to any of these markers compared with that in the PBS group (Figure 5B). However, IL-6 ($P = 0.035$), CXCL1 ($P = 0.02$), and monocyte chemoattractant protein 1 ($P = 0.004$) were increased in these mice (Figure 5C). Additionally, there was a significant increase in Ly6G-positive neutrophil infiltration in the lungs of *E. coli*—exposed pups (Figure 5, D and E) ($P = 0.011$), and the mean airspace area was increased (Supplemental Figure S3, A and B) ($P = 0.0112$). Neutrophil influx and morphologic changes were no longer evident at P7 (Supplemental Figure S3, C and D).

Gut

In the gut, Tnfa ($P = 0.007$), Cxcl1 ($P = 0.031$), and Cxcl2 ($P = 0.038$) mRNA expression levels were elevated, but there was no impact on Il1b, Il6, or Il10 mRNA expression or on the secretion of inflammatory proteins (Figure 6, A and B).

Maternal AAV8-HBD3 Cervical Gene Therapy Improves Pup Survival but Does Not Increase Gestational Length

To validate the utility of the model, AAV8-HBD3 was administered. First, the effect on PTB was evaluated. The gestational length of infected dams was not increased with maternal AAV8-

Figure 3 Neuropathology is evident in neonates (postnatal day 7) exposed to *Escherichia coli in utero*. **A** and **B:** Inflammatory mediators Il1b and allograft inflammatory factor 1 (Iba1) were up-regulated in the forebrain (**A**), whereas all inflammatory mediators were down-regulated in the mid brain region (**B**). **C** and **D:** The average number of terminal transferase-mediated dUTP nick end labeling $(TUNEL)^+$ cells was increased in most brain regions (**C**), and representative images are shown (**D**). **E** and **F:** $IBA1^+$ cell ramification was reduced in the external capsule (EC) and striatum (Str) of the brain in the *E. coli* group (**E**), and representative images are shown (**F**). **G** and **H:** Glial fibrillary acidic protein (GFAP) was increased in the pyriform cortex (Pyr) and the external capsule (**G**), and representative images are shown (**H**). **I:** The average number of neuronal nuclei $(NeuN)^+$ cells was reduced in the hippocampus (Hip). **J**—**L:** There was no impact on brain width (**J**) or hippocampal volume (**L**), but the cortical thickness was reduced in the *E. coli* group (**K**). **Dashed line boxed areas** denote the regions where the insert image was captured. mRNA: $n = 8$ to 10 from 5 litters (**A** and **B**); immunohistochemistry analyses: $n = 5$ to 7 from 5 litters per group (**C**—**L**). $^*P < 0.05$, $^{**}P < 0.01$, $^{***}P < 0.001$, and $^{****}P < 0.0001$. Scale bar = 59.5 μm (**D**, **F**, and **H**). CA, cornu ammonis; IR, immunoreactivity; NS, nonsignificant; OLV, optical luminosity value; PBS, phosphate-buffered saline; Thal, thalamus; Tnfa, tumor necrosis factor alpha; Total, all regions.

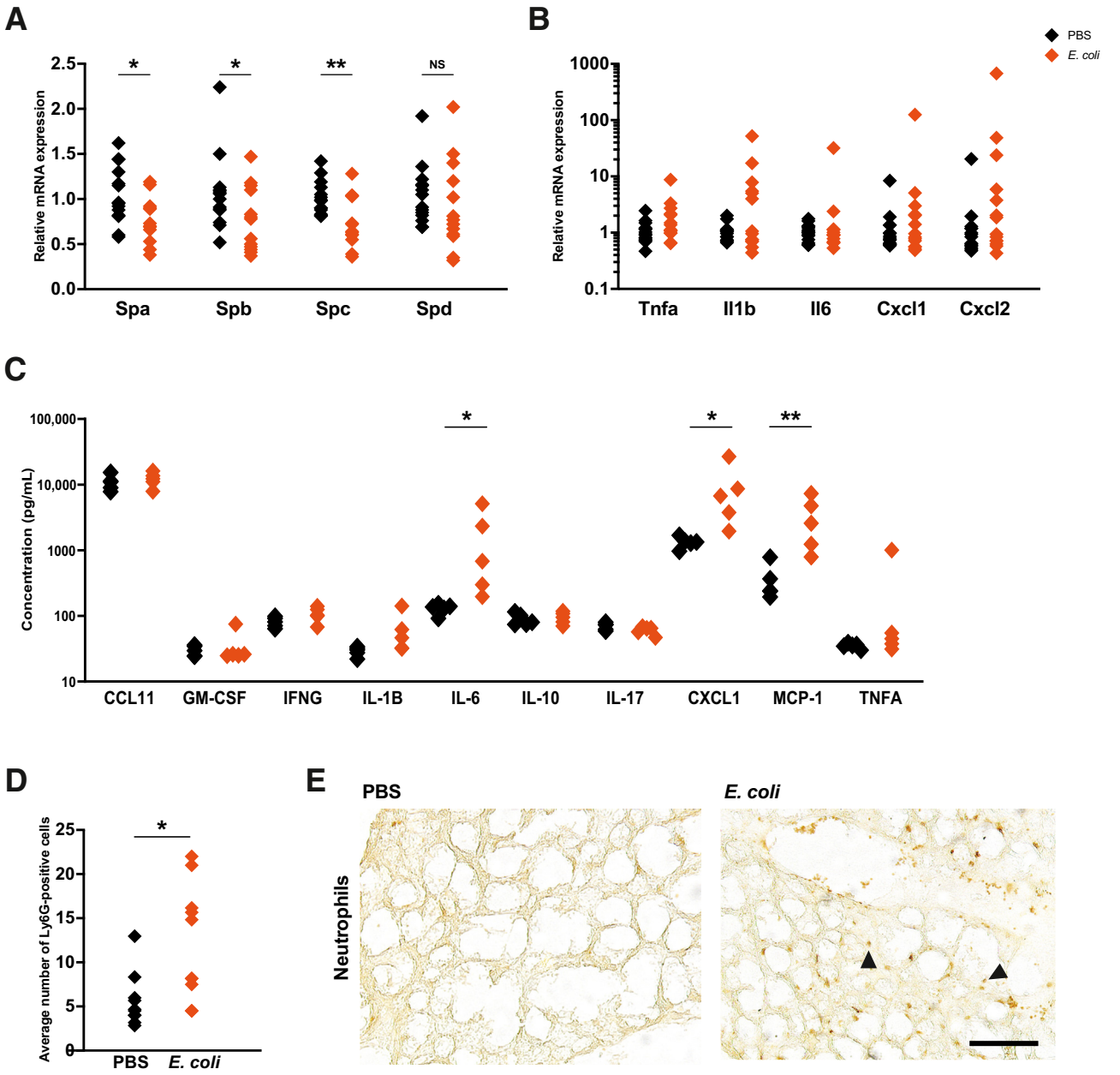

Figure 5 There is evidence of injury to the perinatal lungs following *Escherichia coli* exposure. **A:** Surfactant protein (Sp) mRNA expression was reduced in the *E. coli* group of embryonic day 18.5 pups. **B** and **C:** A trend for increased inflammatory mediator expression could be seen at the mRNA level (**B**), and significant increases were observed at the protein level (**C**). **D** and **E:** The average number of $Ly6G^+$ cells (**black arrowheads**) was increased. $n = 12$ to 15 from 5 litters per group (**B**); $n = 5$ from 5 litters per group (**C**); immunohistochemistry: $n = 10$ from 5 litters per group (**D** and **E**). $^*P < 0.05$, $^{**}P < 0.01$. Scale bar = 59.5 μm (**E**). CCL11, chemokine (C-C motif) ligand 11; GM-CSF, granulocyte-macrophage colony-stimulating factor; IFNG, interferon gamma; MCP-1, monocyte chemoattractant protein 1; NS, nonsignificant; PBS, phosphate-buffered saline; TNFA, tumor necrosis factor alpha.

HBD3 treatment compared with the AAV8-GFP + *E. coli* group (42.54 ± 6 versus 46.55 ± 5 hours, respectively) (Figure 7A). The percentage of live-born pups was significantly increased in comparison to the AAV8-GFP + *E. coli* group (Figure 7B) (85.2% versus 58.6%, respectively; $P = 0.043$), and pup survival was improved over 7 days (Figure 7C) ($P = 0.002$). This is consistent with previous data using this treatment.[19]

This model was also used to examine the therapeutic effect on perinatal brain pathology. AAV8-HBD3 reduced Tnfa mRNA expression in the E18.5 pup brains exposed to *E. coli* compared with control vector ($P = 0.008$; Figure 7D) but did not significantly alter Il1b or Il6 mRNA expression (Figure 7, E and F).

Discussion

PTB, and the resulting neonatal morbidity and mortality, is a serious global health issue for which preventative treatments are largely ineffective. It is essential to establish clinically

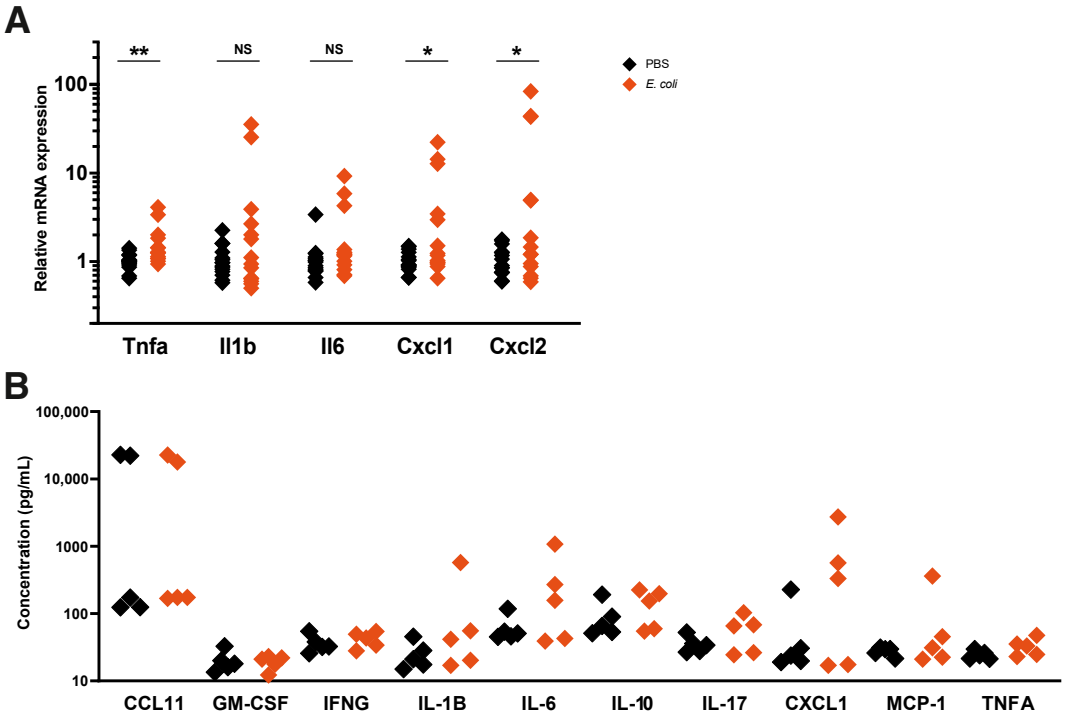

Figure 6 *Escherichia coli* induces perinatal gut inflammation. **A:** Inflammatory mediator mRNA expression was increased in the gut. **B:** There was no change to the protein expression of these mediators. $n = 14$ to 15 from 5 litters per group (**A**); $n = 5$ from 5 litters per group (**B**). $^{*}P < 0.05$, $^{**}P < 0.01$. CCL11, chemokine (C-C motif) ligand 11; GM-CSF, granulocyte-macrophage colony-stimulating factor; IFNG, interferon gamma; MCP-1, monocyte chemoattractant protein 1; NS, nonsignificant; PBS, phosphate-buffered saline; TNFA, tumor necrosis factor alpha.

relevant models to recapitulate not only preterm delivery but also the impact this has on the fetus to develop innovative interventions. It is possible to replicate ascending vaginal infection in mice.[18] Here, neuropathology, lung injury, and gut inflammation, key neonatal morbidities associated with prematurity, were modeled. Furthermore, this model was used to investigate cervical gene delivery of HBD3, revealing that this intervention can significantly increase pup survival while reducing Tnfa expression in the perinatal brain.

Modeling Ascending Vaginal Infection and PTB

This mouse model is the only one, to our knowledge, that recapitulates the human condition, whereby PTB is induced by live bacterial ascending infection, that also reduces pup survival and causes neonatal morbidity in the survivors. Mice are commonly used to model human PTB. There are several methods used to induce labor, but by far the most common method is via lipopolysaccharide (LPS) administration.[25] However, there is huge heterogeneity among models, which differ in the mouse strain used, LPS serotype, LPS dose, mode of delivery, and day of induction.[26] LPS models have several disadvantages. The use of a bacterial product rather than live bacteria means it is a model of inflammation, not infection, and the clinical scenario of ascension through the cervix cannot be recapitulated because of LPS immotility. In addition, the dose required to induce PTB is often lethal for fetuses, preventing neonatal morbidity studies.[27]

Recently, another study characterized a similar model of *E. coli*–induced PTB, demonstrating bacterial ascension, maternal inflammation, and early delivery, validating the current results. However, regardless of *E. coli* dose, there were no surviving pups.[28,29] In a later study, this group reported 47.1% live-born pups when combining the vaginal delivery of a low dose of *Ureaplasma parvum* and *E. coli*. However, neonatal outcomes were not assessed.[30] Others have modeled ascending infection with bacteria of particular relevance to human PTB, such as *U. parvum* and Group B *Streptococcus*.[31–35] However, these bacteria do not consistently induce labor in mice, and the impact on pups has not been investigated beyond recording survival immediately after birth. Although *E. coli* is not a common organism implicated in PTB, it is associated with preterm sequelae in mothers and is often associated with poor neonatal outcomes.[36–38] Specifically, *E. coli* K1 strains are commonly acquired from the mother at birth and are associated with neonatal sepsis and meningitis.[39] Indeed, the dams can often become unwell with this pathogenic strain. However, they usually recover following parturition.

Neuropathology

Markers of neuroinflammation were evident during the perinatal period at both the mRNA and protein level in pups exposed to *E. coli*, which is in agreement with mouse models of intrauterine inflammation induced by LPS.[40–46]

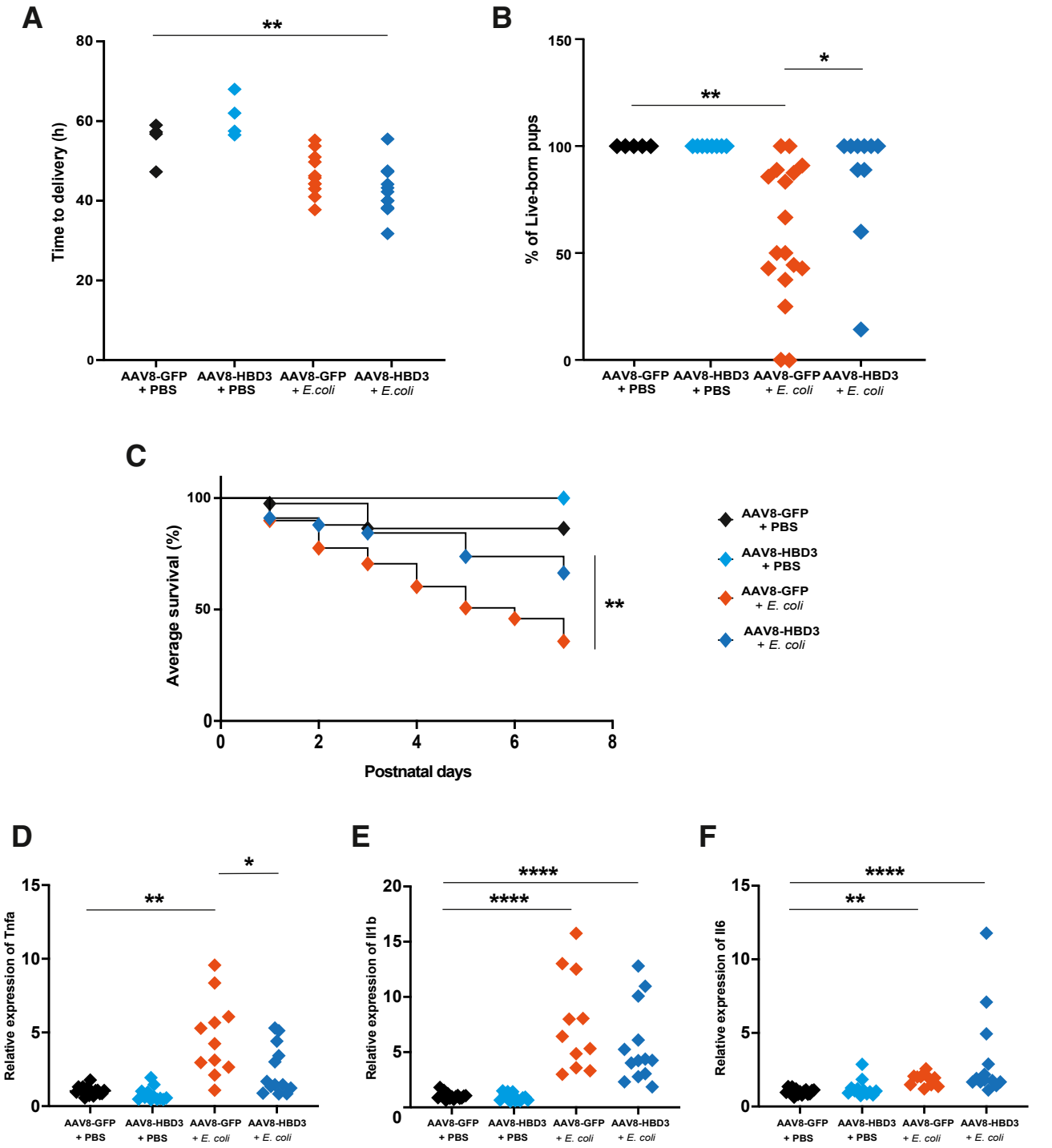

Figure 7 Cervical human β defensin 3 (HBD3) gene delivery improves pup survival and reduces tumor necrosis factor alpha (Tnfa) in the perinatal brain. **A**–**C:** HBD3 treatment did not impact the length of gestation (**A**), but increased the percentage of live-born pups (**B**) and long-term pup survival (**C**). **D**–**F:** Tnfa, but not Il1b and Il6, was reduced in the perinatal brain following maternal cervical HBD3 gene delivery. Delivery and survival: adeno-associated virus 8 (AAV8)–green fluorescent protein (GFP) + phosphate-buffered saline (PBS) $n = 5$ litters, AAV8-HBD3 + PBS $n = 8$ litters, AAV8-GFP + *Escherichia coli* $n = 17$ litters, AAV8-HBD3 + *E. coli* $n = 10$ litters (**A**–**C**); mRNA: $n = 11$ to 15 from 5 litters per group (**D**–**F**). *$P < 0.05$, **$P < 0.01$, and ****$P < 0.0001$.

The developing brain is extremely sensitive to inflammation; an adverse environment even in an asymptomatic mother could cause brain injury in the fetus, and cytokines are known to be neurotoxic.[47] Maternal infection and inflammation may alter the permeability of the fetal blood-brain barrier, leading to neuroinflammation. Through exposure to excess inflammatory mediators, immune cells can accumulate at the embryonic choroid plexus, weakening tight junctions at this barrier.[48] It is hypothesised that the neuroinflammation is due to systemic inflammation and

potentially infection in the pups. Evidence of *E. coli* in the gastrointestinal and respiratory tracts has been previously published.[18] Although pups were not assessed for infection in this current study, as the *E. coli* K1 strain is associated with meningitis, it is possible that the microbes could cross the blood-brain barrier.

While there was a visible trend for reduced ramification of microglia at E18.5, suggesting phagocytic activity, neuropathology was not fully evident until P7, which is likely the result of this perinatal neuroinflammation. A limitation of this model is the variation seen both within and between litters, where some pups exhibit significantly more inflammatory mediator expression than others. As live bacteria were administered, it was impossible to control the spread of the infection, but the position of fetuses in the uterine horns may also have played a role. In future studies, further exploration is needed to understand the patterns of ascending infection into the uterine horns. It would also be worthwhile to increase the group numbers, so that the true impact of infection can be appreciated.

Only minimal inflammation, restricted to the prefrontal cortex region of the brain, remained by P7, with modest increases in Il1b and the microglial marker, Iba1. Interestingly, mRNA expression of all mediators assessed was reduced in the mid brain region (consisting mainly of the hippocampus, thalamus, and striatum) of these mice. This lack of inflammatory mRNA expression could be the result of substantial apoptosis. There were activated microglia in the hippocampus, evidenced by a phagocytic phenotype, which may be associated with the increased $TUNEL^+$ cell death and reduced neuronal density in this region. Alternatively, both this down-regulation in inflammatory mediators and neuronal density could be explained by the reduction in NF-κB activity. NF-κB is a key modulator of inflammatory genes, but low levels of NF-κB response in the brain are also associated with neuronal apoptosis.[49] In future studies, dissection of individual brain regions would provide a fuller picture of the mRNA expression changes at this time point.

Astrogliosis can occur in response to neuronal loss following central nervous system injury. These cells release cytokines that may exacerbate inflammation and injury, but they also restore homeostasis and promote neurogenesis.[50] However, GFAP staining was not increased in the hippocampus at P7, which could suggest that neurogenesis was not stimulated by astrocytes in this region, resulting in the consistently reduced neuronal density at P7 and P14.

In addition to reduced neurogenesis, activation of both microglia and astroglia was increased across multiple brain regions, which has been reported in intrauterine inflammation models.[51–53] $TUNEL^+$ cell death was evident throughout the brain. White matter injury, periventricular leukomalacia, and cerebral palsy are associated with apoptosis and necrosis in the brain.[54,55] Chorioamnionitis-associated white matter injury is common in preterm infants and is thought to begin *in utero*.[56] It is associated with neuronal cell death, microglial activation, and disruption to oligodendrogenesis, which can result in a myelination deficit.[56,57] In the current model, microglial activation was increased, as was cell death and astrogliosis, in the external capsule at P7, suggesting white matter injury pathognomonic of PTB brain injury.

By P14, measurable cell death or astrogliosis was no longer observed, but neuronal density was still reduced in the hippocampus and the cortex. This suggests that although neuroinflammation may have subsided, there was a lasting effect on neurogenesis. There did not appear to be disruption to myelination at P14; however, there is no report of this change until P30 in the LPS mouse model.[44]

Cortical area was reduced in *E. coli*–exposed pups, similarly to prematurely born humans, where reduced cortical thickness has been described.[58–60] Neuroimaging has confirmed reduced white and gray matter volumes in preterm infants, and the microstructure of the cerebral cortex is altered in regions associated with cognition and sensory and motor function.[61,62] Hippocampal volume was not reduced, contrary to what has been reported from other animal models.[52,63]

Here, exposure to ascending vaginal infection during gestation caused disrupted neurodevelopment, which in humans can lead to cognitive and behavioral issues, with an increased risk of cerebral palsy, attention-deficit/hyperactivity disorder, autism spectrum disorder, and psychiatric issues.[64]

Lung Injury

Fetal lungs are susceptible to injury when exposed to infection and/or inflammation via the amniotic fluid.[65] This results in an influx of neutrophils and increased inflammation and can impact alveolarization and surfactant production.[66] Interestingly, inflammatory mediator mRNA expression was only up-regulated in specific pups in our model. This could be a result of the positioning of the pups within the uterine horns. Nevertheless, certain secreted inflammatory mediators were elevated, and the average number of neutrophils in the lungs was increased, which suggests that a measurable level of inflammation was occurring. Indeed, other models have reported an increase in inflammatory mediators[67–69] and neutrophil influx into the fetal lungs.[69,70]

Pulmonary surfactants, important for reducing surface tension, are essential for respiration.[71] Surfactant protein mRNA expression was reduced in the perinatal pup lungs, which is supported by data from other murine models.[67,72] Surfactant deficiency and lung morphologic disruption can result in respiratory distress syndrome and consequent ventilatory support, which can subsequently increase susceptibility to conditions such as bronchopulmonary dysplasia and chronic lung disease of prematurity.[73] The morphology of the fetal lungs was also disrupted, evidenced by increased airspace area. This has been reported in mouse,

sheep, and nonhuman primate models, and may be the result of activated immune cells in the lung.[68,74–76]

A limitation of using mice to model prenatal lung injury is that alveologenesis occurs postnatally in mice, beginning around P4 and peaking at P7, rather than before term, as in humans and nonhuman primates.[65,77] This could explain why lung maturation does not appear to be accelerated in this model. An additional limitation was the collection and processing of these tissues, as the lungs were not inflated. Nevertheless, our model does appear to mimic the morphologic changes seen in neonatal bronchopulmonary dysplasia models.[78,79]

Gastrointestinal Inflammation

There was a marked increase in inflammatory cytokine mRNA expression in the perinatal gut. This particular strain of *E. coli* is known to colonize the gastrointestinal tract, which has been demonstrated in neonatal rats. The bacteria cross the epithelium of the gut into the systemic circulation and enter the central nervous system by crossing the blood-brain barrier, via choroid plexus epithelium, where they invade the meninges.[39,80,81] One study demonstrated increased gut inflammation and increased gut permeability in naturally preterm pups, showing that, even in the absence of infection, prematurity alone is enough to disrupt the gut.[82]

A neonatal mouse model of NEC describes disruption to the intestinal mucosa and increased Il1b and Cxcl2 expression.[83] As the immune system of premature babies may be underdeveloped or dysregulated, they are susceptible to conditions such as NEC, resulting from an exacerbated inflammatory response to microbial products introduced during feeding.[84] In addition, premature infants have delayed bacterial colonization and reduced microbial diversity in the gut. This can have an effect for up to 4 years following disruption during the perinatal period.[85–87] NEC, itself, can result in brain damage because of increased permeability of the gut caused by damage to the intestinal epithelium, leading to bacterial translocation into the blood. The activation of T cells or neurotoxic levels of IFN-γ can activate microglia and lead to disrupted myelination.[88] Although NEC is believed to be established postnatally, we may be modelling a similar pathology. In addition, the colonization of the gut postnatally may contribute to the neonatal neuropathology observed.

Validating the Model by Cervical HBD3 Gene Therapy

Advanced therapies like gene delivery may offer an innovative solution for those at risk of preterm delivery, which has proved difficult to prevent and treat. Although gene therapy is still in the relatively early stages of clinical testing and clinical use, there are increasing numbers of trials investigating gene and cell delivery during pregnancy.[89–92] It was hypothesized that facilitating the up-regulation of the antibacterial peptide HBD3 would enhance the immunologic barrier of the cervix, thus protecting the developing fetus from morbidity and mortality. The current model of ascending vaginal infection was used to validate the previous finding that this gene therapy increases the number of live-born pups.[19] These results have been expanded upon, confirming that postnatal pup survival was also improved, and there was a reduction in Tnfa mRNA expression in the perinatal pup brain, suggesting that this treatment may shield pups from the damaging levels of inflammation resulting from maternal infection. Human neonatal brain damage is associated with elevated TNFA in cord blood.[93–95] Activated microglia release TNFA, but these cells can also be activated by TNFA via a positive feedback loop, resulting in sustained activation.[96] Therefore, by reducing Tnfa, this treatment may prevent neuropathology mediated by cytokine toxicity and microgliosis. Although HBD3 gene therapy did not prevent PTB in this model, it played an arguably more important role in improving pup survival and reducing inflammation in the perinatal brain. Therefore, this treatment strategy warrants further investigation, including a full analysis of the neonatal brain to determine whether this therapy protects pups from neuroinflammation and brain cell death in the longer-term.

Conclusion

It is essential to develop clinically relevant animal models, such as the one described here, to investigate the underlying mechanisms leading to PTB and for the advancement of novel therapies. This mouse model of ascending vaginal infection induced PTB and reduced pup survival but, importantly, this model also recapitulated neonatal morbidity. This includes lung injury, gut inflammation, and neonatal neuropathology, all of which are fundamental to the conditions premature babies are susceptible to. This model was also used to investigate novel therapeutics targeting PTB and the associated neonatal morbidities.

Acknowledgment

We thank a consultant neonatologist for advice and discussions.

Author Contributions

A.K.B. conceived and designed the study, acquired, analyzed, and interpreted the data, and wrote the manuscript; K.T. acquired, analyzed, and interpreted the data, and revised the manuscript; N.S. conceived and designed the study, acquired, analyzed, and interpreted the data, and revised the manuscript; L.B., M.M., and R.K. acquired the data; M.H. performed experiments and interpreted the data; S.N.W. conceived and designed the study, analyzed and interpreted the data, and revised the manuscript; and D.P.

conceived and designed the study, interpreted the data, and revised the manuscript.

Disclosure Statement

None declared.

Supplemental Data

Supplemental material for this article can be found at *http://doi.org/10.1016/j.ajpath.2025.01.008*.

References

1. WHO: recommended definitions, terminology and format for statistical tables related to the perinatal period and use of a new certificate for cause of perinatal deaths: modifications recommended by FIGO as amended October 14, 1976. Acta Obstet Gynecol Scand 1977, 56: 247−253
2. Liu L, Oza S, Hogan D, Chu Y, Perin J, Zhu J, Lawn JE, Cousens S, Mathers C, Black RE: Global, regional, and national causes of under-5 mortality in 2000-15: an updated systematic analysis with implications for the sustainable development goals. Lancet 2016, 388: 3027−3035
3. Chawanpaiboon S, Vogel JP, Moller AB, Lumbiganon P, Petzold M, Hogan D, Landoulsi S, Jampathong N, Kongwattanakul K, Laopaiboon M, Lewis C, Rattanakanokchai S, Teng DN, Thinkhamrop J, Watananirun K, Zhang J, Zhou W, Gülmezoglu AM: Global, regional, and national estimates of levels of preterm birth in 2014: a systematic review and modelling analysis. Lancet Glob Health 2019, 7:e37−e46
4. United Nations Inter-agency Group for Child Mortality Estimation (UN IGME): Levels & Trends in Child Mortality: Report 2017, Estimates Developed by the UN Inter-agency Group for Child Mortality Estimation. New York, NY, United Nations Children's Fund, 2017
5. Blencowe H, Cousens S, Oestergaard MZ, Chou D, Moller AB, Narwal R, Adler A, Vera Garcia C, Rohde S, Say L, Lawn JE: National, regional, and worldwide estimates of preterm birth rates in the year 2010 with time trends since 1990 for selected countries: a systematic analysis and implications. Lancet 2012, 379:2162−2172
6. Boyle AK, Rinaldi SF, Norman JE, Stock SJ: Preterm birth: inflammation, fetal injury and treatment strategies. J Reprod Immunol 2017, 119:62−66
7. Rubens CE, Sadovsky Y, Muglia L, Gravett MG, Lackritz E, Gravett C: Prevention of preterm birth: harnessing science to address the global epidemic. Sci Transl Med 2014, 6:262sr5
8. Jones HE, Harris KA, Azizia M, Bank L, Carpenter B, Hartley JC, Klein N, Peebles D: Differing prevalence and diversity of bacterial species in fetal membranes from very preterm and term labor. PLoS One 2009, 4:e8205
9. DiGiulio DB, Romero R, Kusanovic JP, Gomez R, Kim CJ, Seok KS, Gotsch F, Mazaki-Tovi S, Vaisbuch E, Sanders K, Bik EM, Chaiworapongsa T, Oyarzun E, Relman DA: Prevalence and diversity of microbes in the amniotic fluid, the fetal inflammatory response, and pregnancy outcome in women with preterm pre-labor rupture of membranes. Am J Reprod Immunol 2010, 64:38−57
10. DiGiulio DB: Diversity of microbes in amniotic fluid. Semin Fetal Neonatal Med 2012, 17:2−11
11. Kindinger LM, Bennett PR, Lee YS, Marchesi JR, Smith A, Cacciatore S, Holmes E, Nicholson JK, Teoh TG, MacIntyre DA: The interaction between vaginal microbiota, cervical length, and vaginal progesterone treatment for preterm birth risk. Microbiome 2017, 5:6
12. Bayar E, Bennett PR, Chan D, Sykes L, MacIntyre DA: The pregnancy microbiome and preterm birth. Semin Immunopathol 2020, 42: 487−499
13. Tabatabaei N, Eren AM, Barreiro LB, Yotova V, Dumaine A, Allard C, Fraser WD: Vaginal microbiome in early pregnancy and subsequent risk of spontaneous preterm birth: a case-control study. BJOG 2019, 126:349−358
14. Mishra A, Lai GC, Yao LJ, Aung TT, Shental N, Rotter-Maskowitz A, et al: Microbial exposure during early human development primes fetal immune cells. Cell 2021, 184:3394−3409.e20
15. Stelzer IA, Urbschat C, Schepanski S, Thiele K, Triviai I, Wieczorek A, Alawi M, Ohnezeit D, Kottlau J, Huang J, Fischer N, Mittrücker HW, Solano ME, Fehse B, Diemert A, Stahl FR, Arck PC: Vertically transferred maternal immune cells promote neonatal immunity against early life infections. Nat Commun 2021, 12:4706
16. Jung E, Romero R, Yeo L, Diaz-Primera R, Marin-Concha J, Para R, Lopez AM, Pacora P, Gomez-Lopez N, Yoon BH, Kim CJ, Berry SM, Hsu CD: The fetal inflammatory response syndrome: the origins of a concept, pathophysiology, diagnosis, and obstetrical implications. Semin Fetal Neonatal Med 2020, 25:101146
17. Humberg A, Fortmann I, Siller B, Kopp MV, Herting E, Göpel W, Härtel C: Preterm birth and sustained inflammation: consequences for the neonate. Semin Immunopathol 2020, 42:451−468
18. Suff N, Karda R, Diaz JA, Ng J, Baruteau J, Perocheau D, Tangney M, Taylor PW, Peebles D, Buckley SMK, Waddington SN: Ascending vaginal infection using bioluminescent bacteria evokes intrauterine inflammation, preterm birth, and neonatal brain injury in pregnant mice. Am J Pathol 2018, 188:2164−2176
19. Suff N, Karda R, Diaz JA, Ng J, Baruteau J, Perocheau D, Taylor PW, Alber D, Buckley SMK, Bajaj-Elliott M, Waddington SN, Peebles D: Cervical gene delivery of the antimicrobial peptide, human beta-defensin (HBD)-3, in a mouse model of ascending infection-related preterm birth. Front Immunol 2020, 11:106
20. Buckley SM, Delhove JM, Perocheau DP, Karda R, Rahim AA, Howe SJ, Ward NJ, Birrell MA, Belvisi MG, Arbuthnot P, Johnson MR, Waddington SN, McKay TR: In vivo bioimaging with tissue-specific transcription factor activated luciferase reporters. Sci Rep 2015, 5:11842
21. Percie du Sert N, Ahluwalia A, Alam S, Avey MT, Baker M, Browne WJ, Clark A, Cuthill IC, Dirnagl U, Emerson M, Garner P, Holgate ST, Howells DW, Hurst V, Karp NA, Lazic SE, Lidster K, MacCallum CJ, Macleod M, Pearl EJ, Petersen OH, Rawle F, Reynolds P, Rooney K, Sena ES, Silberberg SD, Steckler T, Würbel H: Reporting animal research: explanation and elaboration for the ARRIVE guidelines 2.0. PLoS Biol 2020, 18:e3000411
22. Cronin M, Akin AR, Collins SA, Meganck J, Kim JB, Baban CK, Joyce SA, van Dam GM, Zhang N, van Sinderen D, O'Sullivan GC, Kasahara N, Gahan CG, Francis KP, Tangney M: High resolution in vivo bioluminescent imaging for the study of bacterial tumour targeting. PLoS One 2012, 7:e30940
23. Hristova M, Cuthill D, Zbarsky V, Acosta-Saltos A, Wallace A, Blight K, Buckley SM, Peebles D, Heuer H, Waddington SN, Raivich G: Activation and deactivation of periventricular white matter phagocytes during postnatal mouse development. Glia 2010, 58: 11−28
24. Möller JC, Klein MA, Haas S, Jones LL, Kreutzberg GW, Raivich G: Regulation of thrombospondin in the regenerating mouse facial motor nucleus. Glia 1996, 17:121−132
25. McCarthy R, Martin-Fairey C, Sojka DK, Herzog ED, Jungheim ES, Stout MJ, Fay JC, Mahendroo M, Reese J, Herington JL, Plosa EJ, Shelton EL, England SK: Mouse models of preterm birth: suggested assessment and reporting guidelines. Biol Reprod 2018, 99:922−937
26. Miller FA, Sacco A, David AL, Boyle AK: Interventions for infection and inflammation-induced preterm birth: a preclinical systematic review. Reprod Sci 2023, 30:361−379
27. Migale R, Herbert BR, Lee YS, Sykes L, Waddington SN, Peebles D, Hagberg H, Johnson MR, Bennett PR, MacIntyre DA: Specific

lipopolysaccharide serotypes induce differential maternal and neonatal inflammatory responses in a murine model of preterm labor. Am J Pathol 2015, 185:2390–2401
28. Spencer NR, Radnaa E, Baljinnyam T, Kechichian T, Tantengco OAG, Bonney E, Kammala AK, Sheller-Miller S, Menon R: Development of a mouse model of ascending infection and preterm birth. PLoS One 2021, 16:e0260370
29. Kammala AK, Mosebarger A, Radnaa E, Rowlinson E, Vora N, Fortunato SJ, Sharma S, Safarzadeh M, Menon R: Extracellular vesicles-mediated recombinant IL-10 protects against ascending infection-associated preterm birth by reducing fetal inflammatory response. Front Immunol 2023, 14:1196453
30. Tantengco OAG, Richardson LS, Radnaa E, Kammala AK, Kim S, Medina PMB, Han A, Menon R: Exosomes from ureaplasma parvum-infected ectocervical epithelial cells promote feto-maternal interface inflammation but are insufficient to cause preterm delivery. Front Cell Dev Biol 2022, 10:931609
31. Pavlidis I, Spiller OB, Sammut Demarco G, MacPherson H, Howie SEM, Norman JE, Stock SJ: Cervical epithelial damage promotes Ureaplasma parvum ascending infection, intrauterine inflammation and preterm birth induction in mice. Nat Commun 2020, 11:199
32. Vornhagen J, Armistead B, Santana-Ufret V, Gendrin C, Merillat S, Coleman M, Quach P, Boldenow E, Alishetti V, Leonhard-Melief C, Ngo LY, Whidbey C, Doran KS, Curtis C, Waldorf KMA, Nance E, Rajagopal L: Group B streptococcus exploits vaginal epithelial exfoliation for ascending infection. J Clin Invest 2018, 128: 1985–1999
33. Bernardini R, Aufieri R, Detcheva A, Recchia S, Cicconi R, Amicosante M, Montesano C, Rossi P, Tchidjou HK, Petrunov B, Orefici G, Mattei M: Neonatal protection and preterm birth reduction following maternal group B streptococcus vaccination in a mouse model. J Matern Fetal Neonatal Med 2017, 30:2844–2850
34. Tantengco OAG, Richardson LS, Radnaa E, Kammala AK, Kim S, Medina PMB, Han A, Menon R: Modeling ascending ureaplasma parvum infection through the female reproductive tract using vagina-cervix-decidua-organ-on-a-chip and feto-maternal interface-organ-on-a-chip. FASEB J 2022, 36:e22551
35. Randis TM, Gelber SE, Hooven TA, Abellar RG, Akabas LH, Lewis EL, Walker LB, Byland LM, Nizet V, Ratner AJ, Group B: Streptococcus [beta]-hemolysin/cytolysin breaches maternal-fetal barriers to cause preterm birth and intrauterine fetal demise in vivo. J Infect Dis 2014, 210:265–273
36. McDonald HM, O'Loughlin JA, Jolley P, Vigneswaran R, McDonald PJ: Vaginal infection and preterm labour. Br J Obstet Gynaecol 1991, 98:427–435
37. Mendz GL, Kaakoush NO, Quinlivan JA: Bacterial aetiological agents of intra-amniotic infections and preterm birth in pregnant women. Front Cell Infect Microbiol 2013, 3:58
38. Min AM, Saito M, Simpson JA, Kennedy SH, Nosten FH, McGready R: Placental histopathology in preterm birth with confirmed maternal infection: a systematic literature review. PLoS One 2021, 16:e0255902
39. McCarthy AJ, Negus D, Martin P, Pechincha C, Oswald E, Stabler RA, Taylor PW: Pathoadaptive mutations of Escherichia coli K1 in experimental neonatal systemic infection. PLoS One 2016, 11: e0166793
40. Brown AG, Maubert ME, Anton L, Heiser LM, Elovitz MA: The tracking of lipopolysaccharide through the feto-maternal compartment and the involvement of maternal TLR4 in inflammation-induced fetal brain injury. Am J Reprod Immunol 2019, 82:e13189
41. Burd I, Bentz AI, Chai J, Gonzalez J, Monnerie H, Le Roux PD, Cohen AS, Yudkoff M, Elovitz MA: Inflammation-induced preterm birth alters neuronal morphology in the mouse fetal brain. J Neurosci Res 2010, 88:1872–1881
42. Burd I, Brown A, Gonzalez JM, Chai J, Elovitz MA: A mouse model of term chorioamnionitis: unraveling causes of adverse neurological outcomes. Reprod Sci 2011, 18:900–907
43. Elovitz MA, Brown AG, Breen K, Anton L, Maubert M, Burd I: Intrauterine inflammation, insufficient to induce parturition, still evokes fetal and neonatal brain injury. Int J Dev Neurosci 2011, 29: 663–671
44. Chang EY, Zhang J, Sullivan S, Newman R, Singh I: N-acetylcysteine attenuates the maternal and fetal proinflammatory response to intrauterine LPS injection in an animal model for preterm birth and brain injury. J Matern Fetal Neonatal Med 2011, 24:732–740
45. Ginsberg Y, Gutzeit O, Hadad S, Divon MY, Khatib N, Fainaru O, Weiner Z, Beloosesky R: Maternal progesterone treatment reduces maternal inflammation-induced fetal brain injury in a mouse model of preterm birth. Reprod Sci 2021, 28:166–176
46. Nadeau-Vallée M, Chin PY, Belarbi L, Brien M, Pundir S, Berryer MH, Beaudry-Richard A, Madaan A, Sharkey DJ, Lupien-Meilleur A, Hou X, Quiniou C, Beaulac A, Boufaied I, Boudreault A, Carbonaro A, Doan ND, Joyal JS, Lubell WD, Olson DM, Robertson SA, Girard S, Chemtob S: Antenatal suppression of IL-1 protects against inflammation-induced fetal injury and improves neonatal and developmental outcomes in mice. J Immunol 2017, 198: 2047–2062
47. McAdams RM, Juul SE: The role of cytokines and inflammatory cells in perinatal brain injury. Neurol Res Int 2012, 2012:561494
48. Cui J, Shipley FB, Shannon ML, Alturkistani O, Dani N, Webb MD, Sugden AU, Andermann ML, Lehtinen MK: Inflammation of the embryonic choroid plexus barrier following maternal immune activation. Dev Cell 2020, 55:617–628.e6
49. Kaltschmidt B, Kaltschmidt C: NF-kappaB in the nervous system. Cold Spring Harb Perspect Biol 2009, 1:a001271
50. Pekny M, Pekna M: Astrocyte reactivity and reactive astrogliosis: costs and benefits. Physiol Rev 2014, 94:1077–1098
51. Hester MS, Tulina N, Brown A, Barila G, Elovitz MA: Intrauterine inflammation reduces postnatal neurogenesis in the hippocampal subgranular zone and leads to accumulation of hilar ectopic granule cells. Brain Res 2018, 1685:51–59
52. Dada T, Rosenzweig JM, Al Shammary M, Firdaus W, Al Rebh S, Borbiev T, Tekes A, Zhang J, Alqahtani E, Mori S, Pletnikov MV, Johnston MV, Burd I: Mouse model of intrauterine inflammation: sex-specific differences in long-term neurologic and immune sequelae. Brain Behav Immun 2014, 38:142–150
53. Lei J, Rosenzweig JM, Mishra MK, Alshehri W, Brancusi F, McLane M, Almalki A, Bahabry R, Arif H, Rozzah R, Alyousif G, Shabi Y, Alhehaily N, Zhong W, Facciabene A, Kannan S, Kannan RM, Burd I: Maternal dendrimer-based therapy for inflammation-induced preterm birth and perinatal brain injury. Sci Rep 2017, 7:6106
54. Volpe JJ: Brain injury in premature infants: a complex amalgam of destructive and developmental disturbances. Lancet Neurol 2009, 8: 110–124
55. Truttmann AC, Ginet V, Puyal J: Current evidence on cell death in preterm brain injury in human and preclinical models. Front Cell Dev Biol 2020, 8:27
56. Anblagan D, Pataky R, Evans MJ, Telford EJ, Serag A, Sparrow S, Piyasena C, Semple SI, Wilkinson AG, Bastin ME, Boardman JP: Association between preterm brain injury and exposure to chorioamnionitis during fetal life. Sci Rep 2016, 6:37932
57. Leviton A, Gressens P: Neuronal damage accompanies perinatal white-matter damage. Trends Neurosci 2007, 30:473–478
58. Nagy Z, Lagercrantz H, Hutton C: Effects of preterm birth on cortical thickness measured in adolescence. Cereb Cortex 2011, 21:300–306
59. Dimitrova R, Pietsch M, Ciarrusta J, Fitzgibbon SP, Williams LZJ, Christiaens D, Cordero-Grande L, Batalle D, Makropoulos A, Schuh A, Price AN, Hutter J, Teixeira RP, Hughes E, Chew A, Falconer S, Carney O, Egloff A, Tournier JD, McAlonan G, Rutherford MA, Counsell SJ, Robinson EC, Hajnal JV, Rueckert D, Edwards AD, O'Muircheartaigh J: Preterm birth alters the development of cortical microstructure and morphology at term-equivalent age. Neuroimage 2021, 243:118488

60. Schmitz-Koep B, Bäuml JG, Menegaux A, Nuttall R, Zimmermann J, Schneider SC, Daamen M, Scheef L, Boecker H, Zimmer C, Gaser C, Wolke D, Bartmann P, Sorg C, Hedderich DM: Decreased cortical thickness mediates the relationship between premature birth and cognitive performance in adulthood. Hum Brain Mapp 2020, 41: 4952−4963
61. Bouyssi-Kobar M, Brossard-Racine M, Jacobs M, Murnick J, Chang T, Limperopoulos C: Regional microstructural organization of the cerebral cortex is affected by preterm birth. Neuroimage Clin 2018, 18:871−880
62. Boardman JP, Counsell SJ: Invited review: factors associated with atypical brain development in preterm infants: insights from magnetic resonance imaging. Neuropathol Appl Neurobiol 2020, 46:413−421
63. Strahle JM, Triplett RL, Alexopoulos D, Smyser TA, Rogers CE, Limbrick DD Jr: Smyser CD: Impaired hippocampal development and outcomes in very preterm infants with perinatal brain injury. Neuroimage Clin 2019, 22:101787
64. Johnson S, Marlow N: Early and long-term outcome of infants born extremely preterm. Arch Dis Child 2017, 102:97−102
65. Jackson CM, Mukherjee S, Wilburn AN, Cates C, Lewkowich IP, Deshmukh H, Zacharias WJ, Chougnet CA: Pulmonary consequences of prenatal inflammatory exposures: clinical perspective and review of basic immunological mechanisms. Front Immunol 2020, 11:1285
66. Wirbelauer J, Schmidt B, Klingel K, Cao L, Lang F, Speer CP: Serum and glucocorticoid-inducible kinase in pulmonary tissue of preterm fetuses exposed to chorioamnionitis. Neonatology 2008, 93:257−262
67. Yavuz A, Sezik M, Eris Yalcin S, Asci H, Ozmen O: Immunohistochemical analysis of protective effects of maternal fingolimod on the placenta and fetal lung and brain in chorioamnionitis-induced preterm birth rat model. Immunopharmacol Immunotoxicol 2020, 42:564−571
68. Papagianis PC, Ahmadi-Noorbakhsh S, Lim R, Wallace E, Polglase G, Pillow JJ, Moss TJ: The effect of human amnion epithelial cells on lung development and inflammation in preterm lambs exposed to antenatal inflammation. PLoS One 2021, 16: e0253456
69. Kallapur SG, Presicce P, Senthamaraikannan P, Alvarez M, Tarantal AF, Miller LM, Jobe AH, Chougnet CA: Intra-amniotic IL-1 [beta] induces fetal inflammation in rhesus monkeys and alters the regulatory T cell/IL-17 balance. J Immunol 2013, 191:1102−1109
70. Hudalla H, Karenberg K, Kuon RJ, Pöschl J, Tschada R, Frommhold D: LPS-induced maternal inflammation promotes fetal leukocyte recruitment and prenatal organ infiltration in mice. Pediatr Res 2018, 84:757−764
71. Meyer KC, Zimmerman JJ: Inflammation and surfactant. Paediatr Respir Rev 2002, 3:308−314
72. Salminen A, Paananen R, Vuolteenaho R, Metsola J, Ojaniemi M, Autio-Harmainen H, Hallman M: Maternal endotoxin-induced preterm birth in mice: fetal responses in toll-like receptors, collectins, and cytokines. Pediatr Res 2008, 63:280−286
73. Davidson LM, Berkelhamer SK: Bronchopulmonary dysplasia: chronic lung disease of infancy and long-term pulmonary outcomes. J Clin Med 2017, 6:4
74. Habelrih T, Tremblay D, Di Battista E, Hou X, Reuben A, Ferri B, Loiselle SE, Côté F, Abram P, Lubell WD, Leimert KB, Quiniou C, Girard S, Olson DM, Chemtob S: Pharmacodynamic characterization of rytvela, a novel allosteric anti-inflammatory therapeutic, to prevent preterm birth and improve fetal/neonatal outcome. Am J Obstet Gynecol 2023, 228:467.e1−467.e16
75. Toth A, Steinmeyer S, Kannan P, Gray J, Jackson CM, Mukherjee S, Demmert M, Sheak JR, Benson D, Kitzmiller J, Wayman JA, Presicce P, Cates C, Rubin R, Chetal K, Du Y, Miao Y, Gu M, Guo M, Kalinichenko VV, Kallapur SG, Miraldi ER, Xu Y, Swarr D, Lewkowich I, Salomonis N, Miller L, Sucre JS, Whitsett JA, Chougnet CA, Jobe AH, Deshmukh H, Zacharias WJ: Inflammatory blockade prevents injury to the developing pulmonary gas exchange surface in preterm primates. Sci Transl Med 2022, 14:eabl8574
76. Stouch AN, McCoy AM, Greer RM, Lakhdari O, Yull FE, Blackwell TS, Hoffman HM, Prince LS: IL-1[beta] and inflammasome activity link inflammation to abnormal fetal airway development. J Immunol 2016, 196:3411−3420
77. Branchfield K, Li R, Lungova V, Verheyden JM, McCulley D, Sun X: A three-dimensional study of alveologenesis in mouse lung. Dev Biol 2016, 409:429−441
78. Durrani-Kolarik S, Pool CA, Gray A, Heyob KM, Cismowski MJ, Pryhuber G, Lee LJ, Yang Z, Tipple TE, Rogers LK: miR-29b supplementation decreases expression of matrix proteins and improves alveolarization in mice exposed to maternal inflammation and neonatal hyperoxia. Am J Physiol Lung Cell Mol Physiol 2017, 313: L339−L349
79. Nguyen L, Castro O, De Dios R, Sandoval J, McKenna S, Wright CJ: Sex-differences in LPS-induced neonatal lung injury. Sci Rep 2019, 9:8514
80. Zelmer A, Bowen M, Jokilammi A, Finne J, Luzio JP, Taylor PW: Differential expression of the polysialyl capsule during blood-to-brain transit of neuropathogenic Escherichia coli K1. Microbiology (Reading) 2008, 154:2522−2532
81. Witcomb LA, Collins JW, McCarthy AJ, Frankel G, Taylor PW: Bioluminescent imaging reveals novel patterns of colonization and invasion in systemic Escherichia coli K1 experimental infection in the neonatal rat. Infect Immun 2015, 83:4528−4540
82. Arboleya S, Rios-Covian D, Maillard F, Langella P, Gueimonde M, Martín R: Preterm delivery: microbial dysbiosis, gut inflammation and hyperpermeability. Front Microbiol 2021, 12:806338
83. Mihi B, Lanik WE, Gong Q, Good M: A mouse model of necrotizing enterocolitis. Methods Mol Biol 2021, 2321:101−110
84. Henderickx JGE, Zwittink RD, van Lingen RA, Knol J, Belzer C: The preterm gut microbiota: an inconspicuous challenge in nutritional neonatal care. Front Cell Infect Microbiol 2019, 9:85
85. Rougé C, Goldenberg O, Ferraris L, Berger B, Rochat F, Legrand A, Göbel UB, Vodovar M, Voyer M, Rozé JC, Darmaun D, Piloquet H, Butel MJ, de La Cochetière MF: Investigation of the intestinal microbiota in preterm infants using different methods. Anaerobe 2010, 16:362−370
86. Arboleya S, Binetti A, Salazar N, Fernández N, Solís G, Hernández-Barranco A, Margolles A, de Los Reyes-Gavilán CG, Gueimonde M: Establishment and development of intestinal microbiota in preterm neonates. FEMS Microbiol Ecol 2012, 79:763−772
87. Fouhy F, Watkins C, Hill CJ, O'Shea CA, Nagle B, Dempsey EM, O'Toole PW, Ross RP, Ryan CA, Stanton C: Perinatal factors affect the gut microbiota up to four years after birth. Nat Commun 2019, 10:1517
88. Zhou Q, Niño DF, Yamaguchi Y, Wang S, Fulton WB, Jia H, Lu P, Prindle T Jr, Pamies D, Morris M, Chen LL, Sodhi CP, Hackam DJ: Necrotizing enterocolitis induces T lymphocyte-mediated injury in the developing mammalian brain. Sci Transl Med 2021, 13: eaay6621
89. Spencer R, Ambler G, Brodszki J, Diemert A, Figueras F, Gratacos E, Hansson SR, Hecher K, Huertas-Ceballos A, Marlow N, Marsal K, Morsing E, Peebles D, Rossi C, Sebire NJ, Timms JF, David AL: EVERREST prospective study: a 6-year prospective study to define the clinical and biological characteristics of pregnancies affected by severe early onset fetal growth restriction. BMC Pregnancy Childbirth 2017, 17:43
90. Herzeg A, Almeida-Porada G, Charo RA, David AL, Gonzalez-Velez J, Gupta N, Lapteva L, Lianoglou B, Peranteau W, Porada C, Sanders SJ, Sparks TN, Stitelman DH, Struble E, Sumner CJ, MacKenzie TC: Prenatal somatic cell gene therapies: charting a path toward clinical applications (proceedings of the CERSI-FDA meeting). J Clin Pharmacol 2022, 62(Suppl 1): S36−S52
91. Schwab ME, Brown JEH, Lianoglou B, Jin C, Conroy PC, Gallagher RC, Harmatz P, MacKenzie TC: Fetal therapies and trials for lysosomal storage diseases: a survey of attitudes of parents and patients. Orphanet J Rare Dis 2022, 17:25

92. Sagar R, David AL: Fetal therapies - (stem cell transplantation; enzyme replacement therapy; in utero genetic therapies). Best Pract Res Clin Obstet Gynaecol 2024, 97:102542
93. Wikström S, Ley D, Hansen-Pupp I, Rosén I, Hellström-Westas L: Early amplitude-integrated EEG correlates with cord TNF-alpha and brain injury in very preterm infants. Acta Paediatr 2008, 97: 915–919
94. Lu HY, Zhang Q, Wang QX, Lu JY: Contribution of histologic chorioamnionitis and fetal inflammatory response syndrome to increased risk of brain injury in infants with preterm premature rupture of membranes. Pediatr Neurol 2016, 61:94–98.e1
95. Lee ES, Kim EK, Shin SH, Choi YH, Jung YH, Kim SY, Koh JW, Choi EK, Cheon JE, Kim HS: Factors associated with neuro-development in preterm infants with systematic inflammation. BMC Pediatr 2021, 21:114
96. Kuno R, Wang J, Kawanokuchi J, Takeuchi H, Mizuno T, Suzumura A: Autocrine activation of microglia by tumor necrosis factor-alpha. J Neuroimmunol 2005, 162:89–96